Micellization Phenomena of Amphiphilic Block Copolymers Based on Methoxy Poly(ethylene glycol) and Either Crystalline or Amorphous Poly(caprolactone-*b*-lactide)

Jie Zhang, Li-Qun Wang,* Hongjun Wang, and Kehua Tu

Institute of Polymer Science, Zhejiang University, Hang Zhou, 310027 China

Received February 24, 2006; Revised Manuscript Received May 12, 2006

This study focuses on the aggregation behavior of the biodegradable amphiphilic block copolymers based on methoxy poly(ethylene glycol) (mPEG) as a hydrophilic block and either crystalline poly(caprolactone-*b*-L-lactide) (P(CL-LLA)) or amorphous poly(caprolactone-*b*-D,L-lactide) (P(CL-DLLA)) as a hydrophobic block. These block copolymers have a strong tendency to form micelles in aqueous medium, with very low critical micelle concentrations (CMCs). The CMC of P(CL-LLA)-*b*-mPEG is higher than that of P(CL-DLLA)-*b*-mPEG when the mPEG block has the same molecular weight. Furthermore, the partition equilibrium coefficient (K_v) of pyrene in the micellar solution of P(CL-LLA)-*b*-mPEG copolymer was lower than that of P(CL-DLLA)-*b*-mPEG copolymer when the mPEG block was the same length. These differences were believed to be related to the physical state of the core-forming blocks, i.e., the crystalline P(CL-LLA) block and the amorphous P(CL-DLLA) block. The TEM images showed that micelles formed by P(CL-LLA)-*b*-mPEG assembled in a cylindrical morphology, whereas those formed by P(CL-DLLA)-*b*-mPEG took a classical spherical shape. In addition, with differential scanning calorimetry (DSC) and wide-angle X-ray diffraction (WAXD) analyses, it is believed that the crystallization tendency of the core-forming blocks is the main factor governing the morphology of micelles in water. A possible mechanism for the cylindrical assembly morphology was discussed.

Introduction

It is well-known for decades that when amphiphilic block copolymers are dissolved in a solvent selective for one of the blocks micelles are usually formed with a rather dense core of the insoluble blocks, surrounded by the diffuse outer corona formed from the soluble blocks.[1−3] A large variety of block copolymers have been studied extensively in the past decades, and much information has been gathered.[4−14] Generally, micelles are formed with a spherical core and a swollen hydrophilic shell. For the copolymers with specially designed architecture, the micelles can also assemble into other morphologies, such as rods, cylinders, tubules, and vesicles.[15−23] Such nonspherical morphologies are now actively studied because of their potential application in nanoscience and biomaterials.

For the micelle formation that has been studied to date, block copolymers composed of flexible coil−coil blocks are paid more attention. It is well recognized that the major driving force underlying the micelle formation is the decrease of the free energy of the system. High surface tension between the hydrophobic core and the solvent shows the primary contribution to micelle growth in order to decrease the average area per copolymer. Along with more copolymer chains incorporated into a micelle, the intercorona chain repulsion as well as the chain stretching of the core-forming blocks will increase to minimize the interfacial energy. As a result, an entropy loss will be induced. At this stage, the system turns to thermodynamic stability unless by a reduction of the micelle size or by geometry transition from spheres to cylinders and vesicles, or lamellae, where the stretching degree of core-forming chains becomes lower. The recent series of work by Eisenberg's group demonstrates that varieties of morphologies can be obtained with crew-cut micelle-like aggregates produced by polystyrene-*b*-poly(acrylic acid) and polystyrene-*b*-poly(ethylene oxide) copolymers in which the core-forming blocks are much longer.[24−27] These studies have revealed that various morphologies of micelles are governed by a force balance principally involving three factors, i.e., the stretching entropy of the core-forming blocks, the interfacial energy between the micelle core and the solvent, and the intercorona chain repulsive interactions. For these systems, the minimization of the interfacial energy is balanced more by an increase in the chain stretching of the core block than by an increase of the intercorona chain repulsion. The morphology transition is attributed to the entropy loss from the stretching of core-forming block.

On the other hand, when the insoluble block is a crystalline chain, one would assume that the energy of crystallization is so large that this block must pack in a folded structure. The self-assembly of coil−crystalline block copolymers which contain at least one crystalline block has been another important area of micelle research.[28−30] More recently, it was shown that the crystalline nature of the PFDMS block in organometallic block copolymers plays a pivotal role in the formation of cylindrical micelles.[31] Kimura and co-workers reported the self-organization of PLLA-PEG and PLLA-PEG-PLLA during structural changes from nanoparticles in an aqueous dispersion to band structures on a mica substrate.[32−34] The fine structures of the nanobands were demonstrated to be formed by reorganization of the block copolymers when the particles were cast and heat-treated on a mica substrate. Up to now, the understanding of the factors that control the assembly morphology of amphiphilic block copolymers with a crystalline core structure is still considerably poor, and the improved insight is highly desirable.

This paper reports the studies on the assembly behavior of the biodegradable amphiphilic block copolymers consisting of

* Corresponding author. Phone: +86-571-87952596. Fax: +86-571-87952596. E-mail: lqwang@zju.edu.cn.

10.1021/bm0601732 CCC: $33.50
Published on Web 08/23/2006

methoxy poly(ethylene glycol) (mPEG) as a hydrophilic block and either crystalline poly(caprolactone-*b*-L-lactide) (P(CL-LLA)) or amorphous poly(caprolactone-*b*-D,L-lactide) (P(CL-DLLA)) as a hydrophobic block. Introducing PCL into the hydrophobic block was on the aim of taking advantage of the permeability of drugs with molecular weights of less than 400 Da by PCL,[35−37] besides the biodegradability and biocompatibility of these poly(ester)s considering the further investigation on hydrophobic drug loading and release experiments. Herein, these two poly(caprolactone-*b*-lactide) core-forming blocks have similar molecular weights as well as LA/CL molar ratios. Investigations were focused on the effect of the crystalline nature of the core-forming block on the formation of the micelles, especially on micellar morphologies. We have found that these block copolymers have a strong tendency to form micelles in aqueous medium, with very low critical micelle concentrations (CMCs). DSC and WAXD methods were also used in an attempt to gain insight into the nature of the micellar core formed by P(CL-LA) diblock copolymers. The geometrical parameters (the size and morphology) of the micelles were characterized by dynamic light scattering (DLS) and transmission electron microscopy (TEM) techniques. TEM images showed that the micelles made from P(CL-DLLA)-*b*-mPEG copolymers adopt a spherical shape. In contrast, the micelles arising from P(CL-LLA)-*b*-mPEG copolymers exhibit a cylindrical shape. The crystallization of the core-forming blocks is demonstrated to be the driving force for the cylindrical morphology. Finally, from a thermodynamic point of view, a possible mechanism for the cylindrical assembly morphology was suggested. This study makes a valuable addition to the understanding of the micelle formation of polyester−polyether amphiphilic block copolymers with a crystalline core structure.

Experimental Section

Materials. P(CL-LLA) ($M_{n(GPC)}$= 6614 g/mol, PDI = 1.6) and P(CL-DLLA) ($M_{n(GPC)}$= 8121 g/mol, PDI = 1.4) diblock copolymers were kindly provided by Prof. R. Jerome and Dr. P. Lecomte at the University of Liege (Belgium). The copolymers were prepared by using $Bu_2Sn(OMe)_2$ as initiator, and caprolactone was polymerized first followed by the polymerizaiton of lactide. One of the chain ends of the diblock copolymers was capped with a methyl ester group and the other end with a hydroxyl group. LLA/CL and DLLA/CL molar ratios were calculated from the integration ratio of the bands due to PLA blocks at 5.1 ppm and to PCL blocks at 2.3 ppm to be 10.3/1 and 11.2/1 by ^{1}H NMR measurements, respectively. Methoxy poly(ethylene glycol) (mPEG) with molecular weights of 1100, 2000, and 5000 was purchased from Fluka. The materials were dried in a vacuum at 60 °C for 24 h before use. Dicyclohexylcarbodiimide (DCC) (Acros) was distilled under diminished pressure (bp 130 °C/3 mmHg) prior to use. 4-(*N*,*N*-Dimethylamino) pyridine (DMAP) and succinic anhydride were recrystallized from ethyl acetate and acetic anhydride, respectively. Triethylamine (TEA) was dried with 4A molecular sieve before use. 1,4-Dioxane and methylene chloride were dried over sodium and anhydrous calcium chloride, respectively, and then distilled. All other chemicals were used as received.

Carboxylic-acid-terminal mPEG was prepared according to Zalipsky et al.[38] and You Han Bae et al.[39] Briefly, succinic anhydride (3.6 mmol) and DMAP (3 mmol) were dissolved in 1,4-dioxane (10 mL) in a sealed flask at room temperature. The flask was evacuated three times and filled with nitrogen. Then, dried mPEG (3 mmol) in 1,4-dioxane (30 mL) and triethylamine (3 mmol) in a small volume of 1,4-dioxane was added successively. The reaction was continued for 24 h at room temperature with stirring and nitrogen atmosphere protection. At the completion of the reaction, dioxane was removed in a rotary vacuum evaporator. The residue was dissolved in CCl_4 (30 mL), and the solid was filtered off. The filtrate was precipitated in diethyl ether. After filtration, the product was dried in a vacuum.

The P(CL-LA)-*b*-mPEG block copolymers with different compositions were synthesized according to the literature.[39] Typically, carboxylic-acid-terminated mPEG (0.4 mmol), P(CL-LA) (0.2 mmol), and DMAP (0.04 mmol) were dissolved in methylene chloride (30 mL) in a sealed flask. Under the same anhydrous conditions, DCC (0.4 mmol) in methylene chloride (10 mL) was added to the previous flask. The reaction was continued for 24 h at room temperature. Precipitated dicyclohexylurea (DCU) was removed by filtration. The filtrate was precipitated in diethyl ether, and the product was collected by filtration and then dried in a vacuum at 40 °C.

Unreacted mPEG moiety was removed from the block copolymers by dialysis method. The GPC chromatograms of purified block copolymers showed a unimodal peak (results not shown).

In the following, P(CL-LLA) and P(CL-DLLA) diblock copolymers are abbreviated as C-L and C-DL, respectively. P(CL-LLA)-*b*-mPEG and P(CL-DLLA)-*b*-mPEG amphiphilic block copolymers are respectively abbreviated as (C-L)-E_x and (C-DL)-E_x. The numbers of the subscripts indicate the molecular weight of the corresponding mPEG blocks in hundred g/mol.

Preparation of the Aqueous Micellar Solutions. Since the micelles cannot be prepared by direct dissolution of the resultant block copolymers in water, the aqueous micellar solutions were prepared by a modified procedure described by Zhang et al.[15] Briefly, the block copolymers were first dissolved in *N*,*N*-dimethylformamide (DMF), a solvent for both P(CL-LA) and mPEG blocks. In detail, when preparing micelle solutions for fluorescence measurements, the polymer concentrations in DMF solutions before addition of water were 3.0 mg/mL for (C-L)-E_{11} and (C-DL)-E_{11}, 5.0 mg/mL for (C-L)-E_{20} and (C-DL)-E_{20}, and 8.0 mg/mL for (C-L)-E_{50} and (C-DL)-E_{50}, respectively. When preparing micelle solutions for DLS and TEM measurements, the polymer concentrations in DMF solutions were all 2.0 mg/mL. Subsequently, doubly distilled water was added to the polymer/DMF solutions (10 mL) at a rate of 1 drop every 10 s with vigorous stirring. The addition of water was continued until the water content reached 20−30 wt%, depending on the composition of the block copolymers. The resulting solutions were transferred to dialysis tubes (MWCO = 1200, 3500, and 7000, respectively, depending on the molecular weight of mPEG) and dialyzed against doubly distilled water to remove the organic solvent at 4 °C. After dialysis, the solutions turned slightly opaque, except for (C-DL)-E_{20} and (C-DL)-E_{50}, which exhibited transparent solutions. The samples for DSC and WAXD measurements were prepared by quick freezing in liquid nitrogen and thereafter lyophilized.

Fluorescence Measurements. Fluorescence spectra were recorded on a HITACHI F-4500 fluorescence spectrophotometer. Pyrene was used as a fluorescence probe to analyze the P(CL-LA)-*b*-mPEG block copolymers in doubly distilled water. Samples for fluorescence measurement were prepared according to the literature,[40] and the concentration of the aqueous solutions ranged from 1.0×10^{-6} to 1.5 mg/mL. The pyrene concentration in the solution was chosen to be 6.0×10^{-7} M. For the measurement of pyrene excitation spectra, the slit widths for both excitation and emission sides were maintained at 2.5 nm, and an emission wavelength of 372 nm was used.

Differential Scanning Calorimetry (DSC). DSC experiments were performed using a Perkin Elmer Pyris 1 DSC instrument. The lyophilized samples of P(CL-DLLA)-*b*-mPEG and P(CL-LLA)-*b*-mPEG block copolymers were heated under nitrogen atmosphere from −70 to +170 °C at a heating rate of 10 °C/min.

Wide-Angle X-ray Diffraction (WAXD). The wide-angle X-ray diffraction patterns of the lyophilized samples were recorded at a Rigaku D/max-rA X-ray diffractometer (Japan) with a Cu Kα source (λ= 1.5406 nm; 40 kV; 80mA) in the 2θ range of 5−50° at a scanning speed of 2.0° min^{-1}.

Particle Size Measurements. The hydrodynamic diameter and size distribution of micelles were determined by dynamic light scattering

Table 1. Molecular Characteristics of the P(CL-LA)-*b*-mPEG Block Copolymers

	prepolymers		P(CL-LA)-*b*-mPEG				
samples	mPEG (M_n)[a]	P(CL-LA) (M_n)[a]	M_n[a]	M_w[a]	M_w/M_n[a]	M_n[b]	wt%[c] of hydrophobic block
(C-L)-E_{11}	1146	6614	8882	12501	1.41	7949	89.6
(C-L)-E_{20}	1997	6614	8939	13409	1.50	8287	82.2
(C-L)-E_{50}	5408	6614	10301	14422	1.40	9771	54.5
(C-DL)-E_{11}	1146	8121	9307	11679	1.25	5393	84.5
(C-DL)-E_{20}	1997	8121	9497	11966	1.26	6421	76.6
(C-DL)-E_{50}	5408	8121	10366	13268	1.28	8306	44.1

[a] Measured by GPC analysis. [b] Measured by ^{1}H NMR measurements. [c] Determined on the basis of combination of ^{1}H NMR and GPC results.

(DLS) using a Brookhaven 90 Plus particle size analyzer. Each analysis lasted for three 3 min and was performed at 25 °C with an angle detection of 90°. All micelle solutions had a final polymer concentration of about 0.1 mg/mL. Prior to the light scattering measurements, the sample solutions were filtered through 0.45 μm filters.

In the dynamic light scattering experiments, the measured intensity autocorrelation function of scattered light, $C^{(2)}(t)$, is under standard conditions related to the field autocorrelation function, $C^{(1)}(t)$, by the Siegert relation

$$C^{(2)}(t) = A(C^{(1)}(t))^2 + B \quad (1)$$

where B is the baseline determined for the largest t when all correlation is lost and A is an optical constant determined by the instrument design.

For the case of a monodisperse suspension of rigid, globular particles

$$C^{(1)}(t) = e^{-\Gamma t} \quad (2)$$

$$\Gamma = Dq^2 \quad (3)$$

$$q = 4\pi n \sin(\theta/2)/\lambda \quad (4)$$

Here Γ is related to the relaxation of the fluctuations, D is the translational diffusion coefficient, q is the scattering vector, θ is the scattering angle, λ is the vacuum wavelength of the laser light, and n is the refractive index of the solvent.

From D, a hydrodynamic diameter d_H was determined using the Stokes−Einstein relationship

$$D = k_B T/3\pi\eta d_H \ [\mathrm{cm}^2/\mathrm{s}] \quad (5)$$

which holds for noninteracting spheres. T denotes the absolute temperature, k_B is the Boltzman constant, and η is the solvent viscosity.

In the case of polydisperse systems, a relaxation time distribution $G(\Gamma)$ must be used

$$C^{(1)}(t) = \int G(\Gamma) e^{-\Gamma t}\, d\Gamma \quad (6)$$

where $G(\Gamma)$ is a continuous distribution function of the decay rate Γ from inverse Laplace transformation (ILT) method.[41]

Some expressions do exist for the diffusion coefficient of wormlike or rodlike chains,[42−44] but in this work, we will restrict ourselves to the determination of "equivalent" hydrodynamic diameter, that is, the hydrodynamic diameter that our micelles would have had if they were all spherical.

Transmission Electron Microscopy (TEM). Transmission electron microscopy (TEM) was performed on a JEOL JEM-1230 electron microscope operating at an acceleration voltage of 60 KV. Samples were deposited from micelle solutions with different concentrations (about 0.1 and 0.2 mg/mL) onto copper grids coated with carbon. Water was allowed to evaporate from the grids at atmospheric pressure and 10 °C. The grids were finally negatively stained by 2 wt % phosphotungstic acid (PTA).

Results and Discussion

P(CL-LLA)-*b*-mPEG and P(CL-DLLA)-*b*-mPEG amphiphilic block copolymers were prepared at room temperature by reacting carboxylic-acid-terminal mPEG and hydroxyl-terminated P(CL-LLA) or P(CL-DLLA) in the presence of dicyclohexylcarbodiimide (DCC) as a coupling agent. Along this way, a series of block copolymers with predetermined mPEG, P(CL-LLA), and P(CL-DLLA) blocks were synthesized. The molecular characteristics of the resultant block copolymers are shown in Table 1. Varying predetermined block length of mPEG, P(CL-LLA), and P(CL-DLLA) allows the molecular architecture of the copolymers to be tailored with more flexibility. Furthermore, the choice of P(CL-LLA) and P(CL-DLLA) blocks is based on the aim of modulating the physical properties of the hydrophobic core-forming blocks.

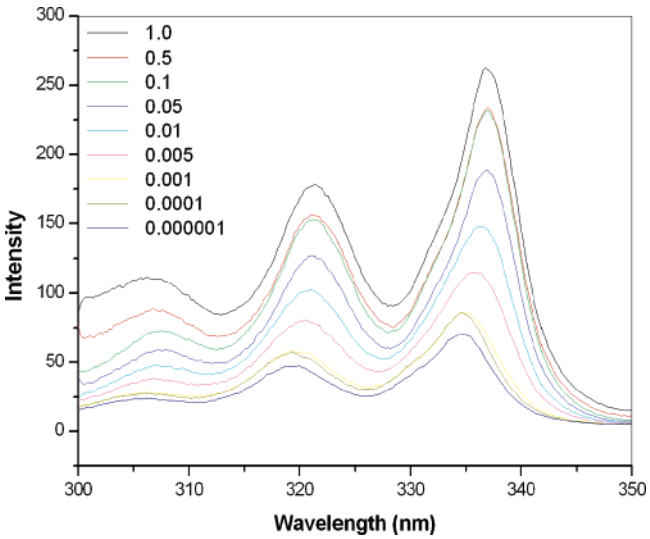

Figure 1. Fluorescence excitation spectra of pyrene as a function of (C-DL)-E_{20} concentration (mg/mL) in water. The concentration of pyrene is 6.0×10^{-7} M.

Critical Micelle Concentration of the Copolymers in Aqueous Medium. The critical micelle concentrations (CMCs) of P(CL-LLA)-*b*-mPEG and P(CL-DLLA)-*b*-mPEG block copolymers with different compositions in aqueous solution were determined by a fluorescence technique using pyrene as a probe. The excitation spectra of pyrene at various concentrations of (C-DL)-E_{20} are shown in Figure 1. The pyrene excitation spectra exhibit a shift from 334.8 to 337.2 nm, indicating the partition of pyrene into the hydrophobic core of the micelles. The shift is utilized to determine the critical aggregation behavior of amphiphilic block copolymers in water. Figure 2, panels a and b, demonstrates the intensity ratios (I_{339}/I_{335}) of pyrene excitation spectra as a function of the logarithm of copolymer concentrations for P(CL-DLLA)-*b*-mPEG and P(CL-LLA)-*b*-mPEG block copolymers with different compositions. At a low concentration range, a negligible change of intensity ratio (I_{339}/I_{335}) is monitored. As the copolymer concentration increases, the intensity ratio exhibits a substantial increase at a certain concentration, suggesting that pyrene molecules are incorporated

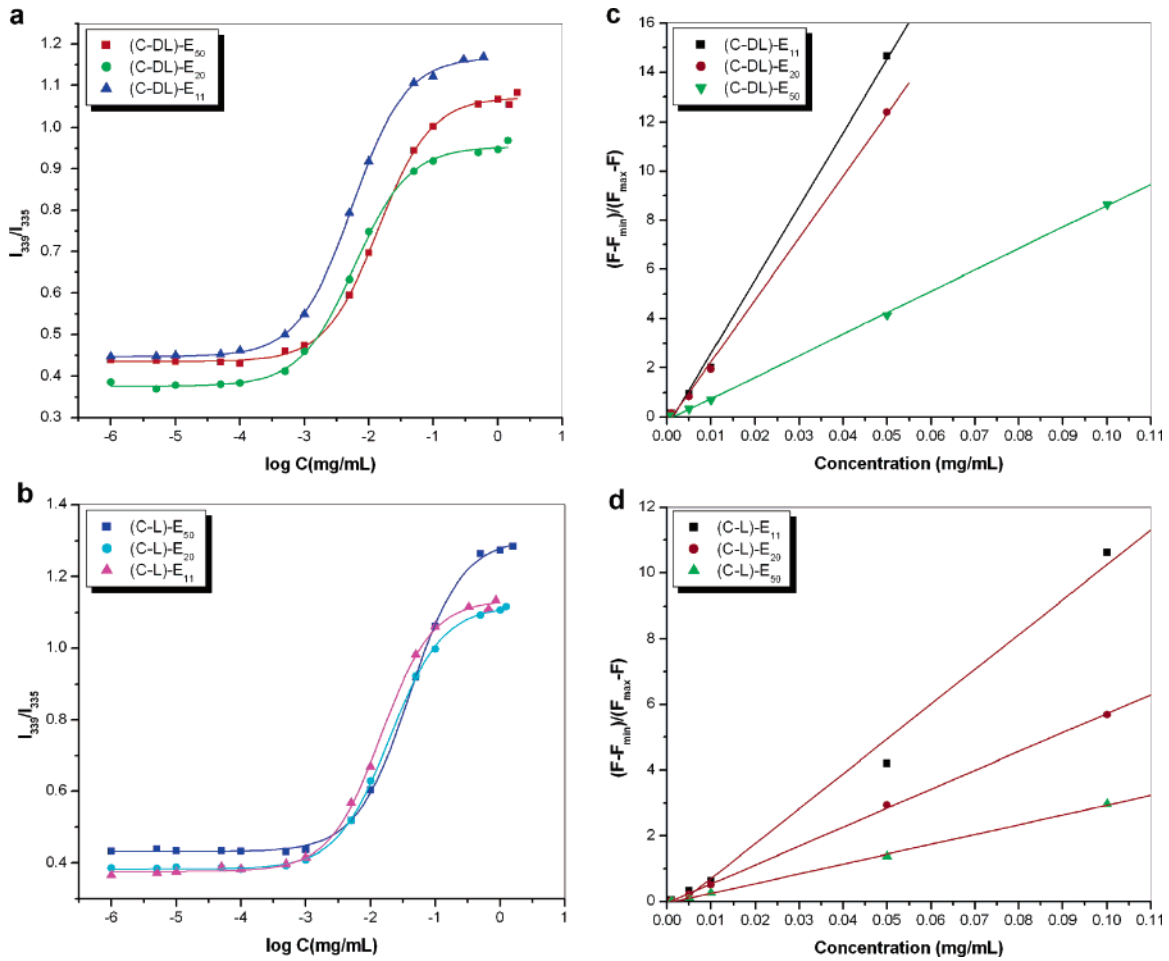

Figure 2. Plots of fluorescence intensity ratio I_{339}/I_{335} from pyrene excitation spectra vs log C for (a) P(CL-DLLA)-*b*-mPEG and (b) P(CL-LLA)-*b*-mPEG block copolymers with different compositions. Plots of $(F - F_{min})/(F_{max} - F)$ vs polymer concentrations for (c) P(CL-DLLA)-*b*-mPEG and (d) P(CL-LLA)-*b*-mPEG block copolymers with different compositions.

Table 2. Micellar Characteristics of the P(CL-LA)-*b*-mPEG Block Copolymers

samples	micelle diameter (nm)[a]	micelle diameter (nm)[b]	ΔH_m (J/g)[d]	CMC (mg/mL)	K_v
(C-L)-E_{11}	32.4 ± 10.7	16.0 ± 1.8[c]	41.2	1.7×10^{-3}	1.24×10^5
(C-L)-E_{20}	66.7 ± 17.2	12.4 ± 0.6[c]	36.4	2.3×10^{-3}	7.32×10^4
(C-L)-E_{50}	43.8 ± 7.4	13.8 ± 1.0[c]	30.6	3.5×10^{-3}	5.72×10^4
(C-DL)-E_{11}	70.7 ± 19.8	59.0 ± 15.9		0.47×10^{-3}	3.79×10^5
(C-DL)-E_{20}	35.4 ± 3.0	14.2 ± 1.6		0.50×10^{-3}	3.53×10^5
(C-DL)-E_{50}	33.7 ± 4.1	12.1 ± 0.9		1.5×10^{-3}	2.12×10^5

[a] Mean diameters by dynamic light scattering (DLS). [b] Number average diameter of the micelles from TEM images. [c] Number average width of the cylindrical micelles from TEM image. [d] Normalized values with respect to the weight% composition, $\Delta H_m = \Delta H_i/w_i$, where ΔH_i is the area of the endothermic peak of P(CL-LLA) block recorded from DSC thermograph and w_i is the weight fraction of the corresponding block.

into the hydrophobic core region upon micelle formation. The critical micelle concentrations are therefore determined from the crossover point at the low concentration range.

The CMC values of P(CL-LLA)-*b*-mPEG and P(CL-DLLA)-*b*-mPEG block copolymers with different compositions are listed in Table 2. It can be found that the CMC of P(CL-DLLA)-*b*-mPEG is lower than that of P(CL-LLA)-*b*-mPEG when the mPEG block with the same molecular weight, e.g., 0.47×10^{-3} mg/mL for (C-DL)-E_{11} vs 1.7×10^{-3} mg/mL for (C-L)-E_{11}. However, for both cases of P(CL-DLLA)-*b*-mPEG and P(CL-LLA)-*b*-mPEG, higher CMC values are observed when the hydrophilic mPEG composition becomes higher. It is also found that the CMC values of these copolymers are quite low in contrast to those of other amphiphilic block copolymers reported in the literature,[8,45−48] indicating that the block copolymers in this study possess strong thermodynamic stability in aqueous solution and could perform as favorable drug carriers in our ongoing experiments on the drug loading characteristics.

Partition of Pyrene in the Micellar Solutions. The partition equilibrium constant (K_v) of a hydrophobic probe, pyrene, in the micellar solution is calculated using the method of Wilhelm et al.[40] and Lee et al.,[47,48] in which pyrene distributing into the micelles is considered as a simple equilibrium between a micellar phase of volume V_m and a water phase of volume V_w. Thus, the ratio of pyrene in the micellar phase to the water phase $[Py]_m/[Py]_w$ can be expressed as the volume ratio of the two phases according to eq 7

$$[Py]_m/[Py]_w = K_v V_m/V_w \quad (7)$$

Equation 7 can be rewritten as

$$[\mathrm{Py}]_m/[\mathrm{Py}]_w = K_v XC/1000\rho \quad (8)$$

where X is the weight fraction of hydrophobic P(CL-LA) in the block copolymer, C is the copolymer concentration, and ρ is the density of P(CL-LA) core of micelles, which is approximated as the density of bulk ($\rho_{C-L} = 1.045$, $\rho_{C-DL} = 1.073$).

The intermediate range of copolymer concentrations permits calculation of the ratio ($[\mathrm{Py}]_m/[\mathrm{Py}]_w$) of the pyrene as

$$[\mathrm{Py}]_m/[\mathrm{Py}]_w = (F - F_{min})/(F_{max} - F) \quad (9)$$

where F_{min} and F_{max} are the average I_{339}/I_{335} ratios in the flat regions of the low and high concentration ranges in the I_{339}/I_{335} versus log copolymer concentration plots, and F is the intensity ratio (I_{339}/I_{335}) in the intermediate concentration range. Thus, K_v is obtained from the slope of a plot of $(F - F_{min})/(F_{max} - F)$ vs copolymer concentration (Figure 2, panels c and d) and listed in Table 2. It can be seen that the K_v value of P(CL-LLA)-*b*-mPEG micelles is lower than that of P(CL-DLLA)-*b*-mPEG with a mPEG block of the same molecular weight, e.g., 5.72×10^4 for (C-L)-E_{50} vs 2.12×10^5 for (C-DL)-E_{50}. Since the weight percentage of hydrophobic block for the P(CL-LLA)-*b*-mPEG is even appreciably higher than that for the P(CL-DLLA)-*b*-mPEG system when the hydrophilic block is of the same length, the decrease in K_v values for P(CL-LLA)-*b*-mPEG micelles should be explained in terms of the core's physical structure, in which a more tightly packed core would restrain the partition of pyrene in the region. Considering that these copolymers are aimed at performing as drug delivery carries, it is worthwhile to explore the physical state of the micelle core as well as the morphology of the carriers as another performance related physical parameter.

Thermal Analysis and Wide-Angle X-ray Diffraction Studies of the Micelles. In an attempt to gain insight into the physical state of the micelle cores, differential scanning calorimetry (DSC) and wide-angle X-ray diffraction (WAXD) studies of the lyophilized micelles were carried out. DSC thermograms are shown in Figure 3. In all cases of the micelles formed from three P(CL-LLA)-*b*-mPEG copolymers, two melting peaks are observed in the heating thermograms. The lower melting peaks are assigned to mPEG blocks, and the subsequent melting peak at about 150 °C is attributed to P(CL-LLA) blocks. Because the thermograms are obtained directly from the first heating run, it is believed that the information of thermal history coming from the micelle formation is revealed. The appearance of mPEG melting peaks should be the result of the crystallization of mPEG block in the lyophilizing procedure at −40 °C because of the low T_gs of mPEG blocks (ca. −60 °C). Since the temperature of the freeze-drying procedure (−40 °C) is much lower than the glass transition temperature of P(CL-LLA) (30 °C), the melting peak assigned to P(CL-LLA) blocks is believed to be the result of the crystallization of P(CL-LLA) core-forming blocks during micellization.

In contrast, only the melting peaks corresponding to mPEG blocks are observed in the DSC thermograms of the micelle samples from P(CL-DLLA)-*b*-mPEG copolymers, indicating the amorphous nature of micelle cores formed by P(CL-DLLA) blocks.

A similar illustration is obtained from the WAXD patterns in Figure 4. The peak in the pattern of the micelles formed by (C-L)-E_{50} has a *d* spacing of 5.34 Å, which is closely matching with that of the bulk P(CL-LLA). While the pattern of the micelles formed by (C-DL)-E_{50} only exhibits the peaks of mPEG with the *d* spacing of 4.66 and 3.82 Å.

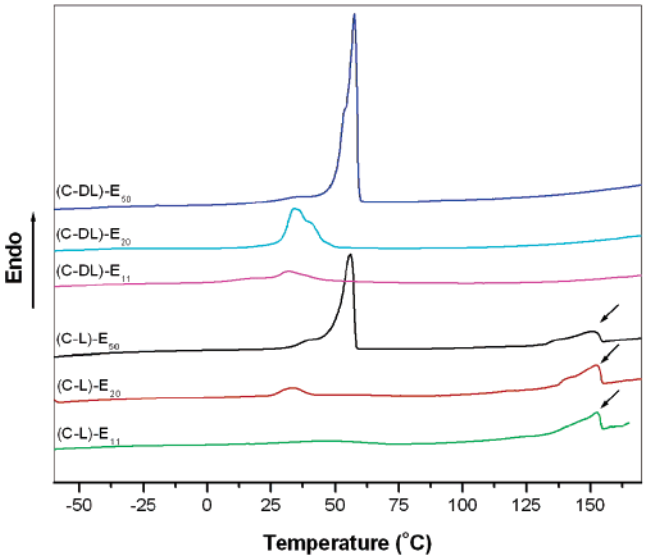

Figure 3. DSC heating curves of the lyophilized micelles.

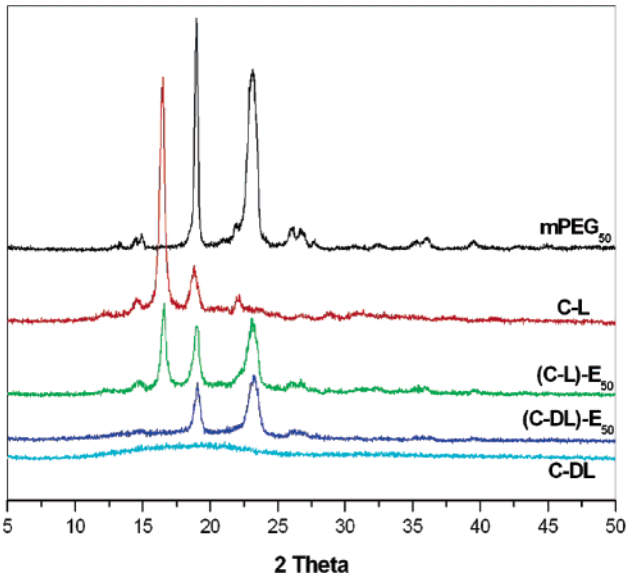

Figure 4. WAXD patterns of the lyophilized (C-L)-E_{50} and (C-DL)-E_{50} micelles.

Hydrodynamic Diameters in Aqueous Solution. It has been known that the more hydrophobic the micellar core is, the more copolymer chains are aggregated into a micelle in order to minimize the interfacial energy. Therefore, the size of the constructed micelles is larger. In agreement with this principle, one can find that the hydrodynamic diameters of the micelles formed by (C-DL)-E_{11} are larger than those of (C-DL)-E_{20} and (C-DL)-E_{50} (Table 2). With the increase of hydrophilic mPEG block length and thus the elevated stability, the aggregation number of the copolymers into a micelle decreases, resulting in the decrease in micellar size.

However, for the micelles constructed from P(CL-LLA)-*b*-mPEG copolymers with three different mPEG block lengths, the micellar sizes do not seem to follow the principle above.

Morphology and Micelle Size. Figure 5 shows the TEM images of the micelles made from P(CL-DLLA)-*b*-mPEG copolymers. It can be seen that the micelles take a spherical shape regardless of the mPEG length. The size values estimated by TEM are relatively smaller than those obtained from the DLS measurements (Table 2). This is believed to be due to the presence of water in the DLS experiments which inducing the

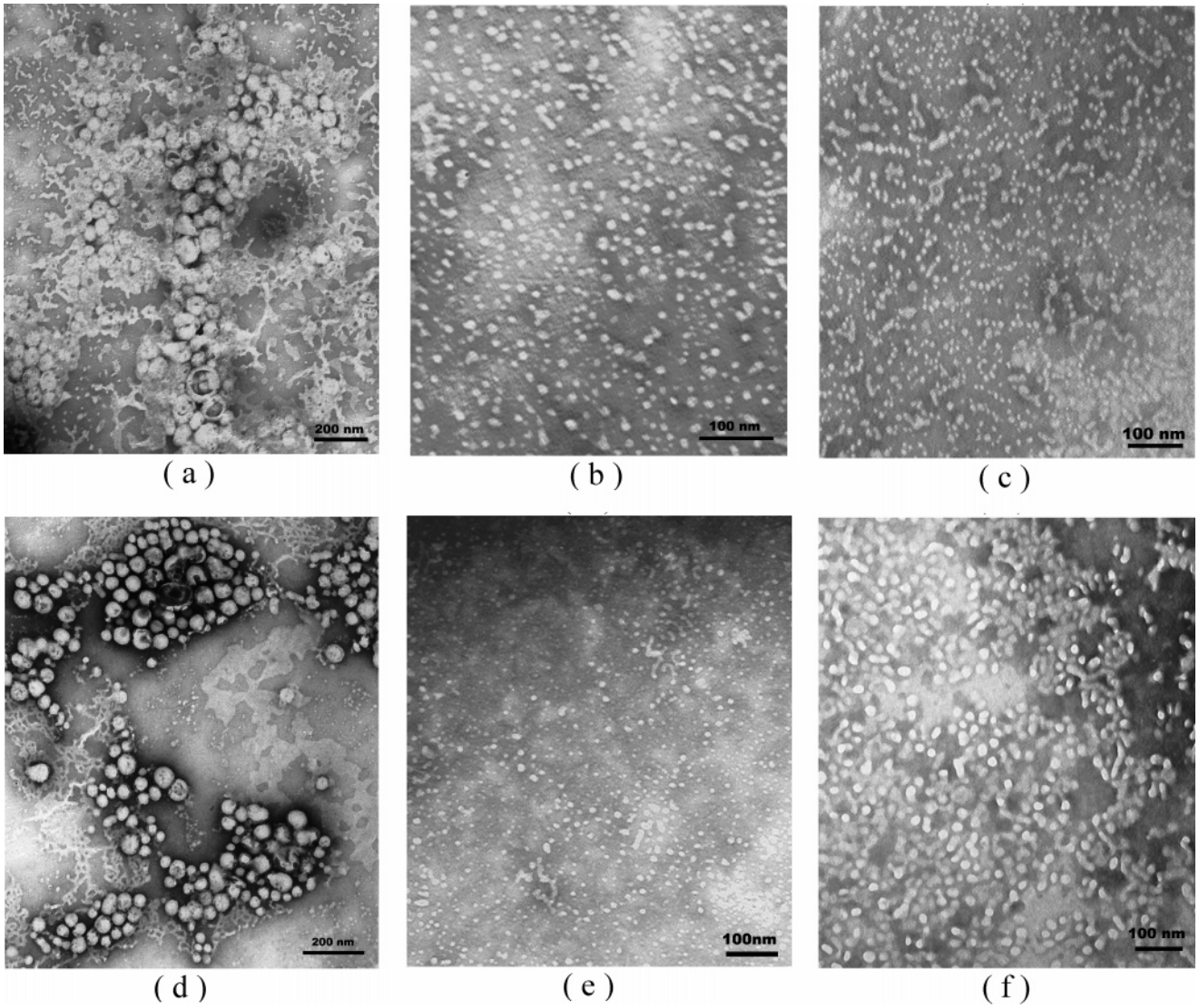

Figure 5. TEM images of spherical micelles from P(CL-DLLA)-*b*-mPEG block copolymers: (a, d) (C-DL)-E_{11}, (b, e) (C-DL)-E_{20}, and (c, f) (C-DL)-E_{50} with concentrations of (a, b, c) 0.1 and (d, e, f) 0.2 mg/mL in water.

swelling of the hydrated mPEG corona. However, it is important to note that the size-changing trend in TEM images is in good agreement with the results of DLS measurements. Generally, the size of micelles decreases as the hydrophilic mPEG block length increases. So it is inferred from this result that the molecular weight of the hydrophilic block plays a dominant role on the size of the micelles derived from P(CL-DLLA)-*b*-mPEG.

A totally different morphology of the micelles constructed by P(CL-LLA)-*b*-mPEG copolymers is presented by TEM measurement, where the aggregation of the copolymers exhibits a cylindrical shape (Figure 6). The width of the micelles in all cases is found to be ca. 10∼20 nm, with lengths varying from 50 nm to several hundred nanometers. The increase of mPEG block length herein does not show so visible an effect on the size of the micelles as in the case of P(CL-DLLA)-*b*-mPEG (Table 2). It is worth noting that the size of the cylindrical micelles measured by TEM cannot be directly compared with that obtained from DLS, since the basic equations to calculate the hydrodynamic diameter (*d*) in DLS measurement are originated from the correlation function cumulant analysis, which is based on the assumption that the particles are noninteracting spheres and not anisotropic objects. Cylindrical micelles may interact differently, for example, entangle with each other, so expressions for the diffusion coefficient of nonspherical model should be utilized.

The effect of the copolymer concentration on the cylindrical micelle morphology is further evaluated. The micellar morphologies of (C-L)-E_{50} copolymer with two different concentrations are illustrated in Figure 7. Magnification of one region reveals that, by increasing the copolymer concentration from 0.1 to 0.2 mg/mL, the cylindrical micelles show more ordered parallel alignment with each other. On the other hand, the width of the micelles from higher concentration is found to be 14.8 ± 1.4 nm, where only a minute increase is exhibited when compared to that of lower concentration sample with 13.8 ± 1.0 nm. This observation implies that the micelles are extended remarkably with the increase of the solution concentration. Based on the results of thermal analysis above, it is believed that the high enthalpy of crystallization of P(CL-LLA) core-forming block combining with its hydrophobicity in aqueous medium is the driving force for the cylindrical morphology.

Proposed Mechanism for the Cylindrical Morphology. The scaling model of Vilgis and Halperin (VH) provides a theoretical foundation for understanding the formation of cylindrical micelles in this study.[28] VH consider a crystalline−coil A−B diblock copolymer that aggregates in a highly B-selective solvent, forming micelles with a chain-folded crystalline core

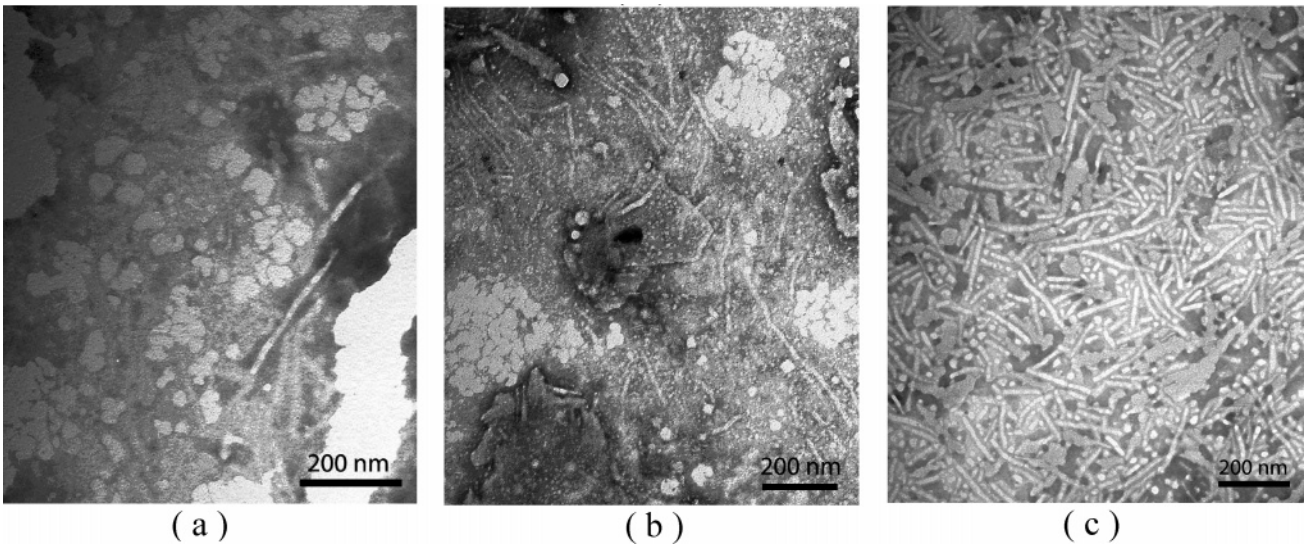

Figure 6. TEM images of cylindrical micelles from P(CL-LLA)-*b*-mPEG block copolymers: (a) (C-L)-E_{11}, (b) (C-L)-E_{20}, and (c) (C-L)-E_{50} with concentrations of 0.1 mg/mL in water.

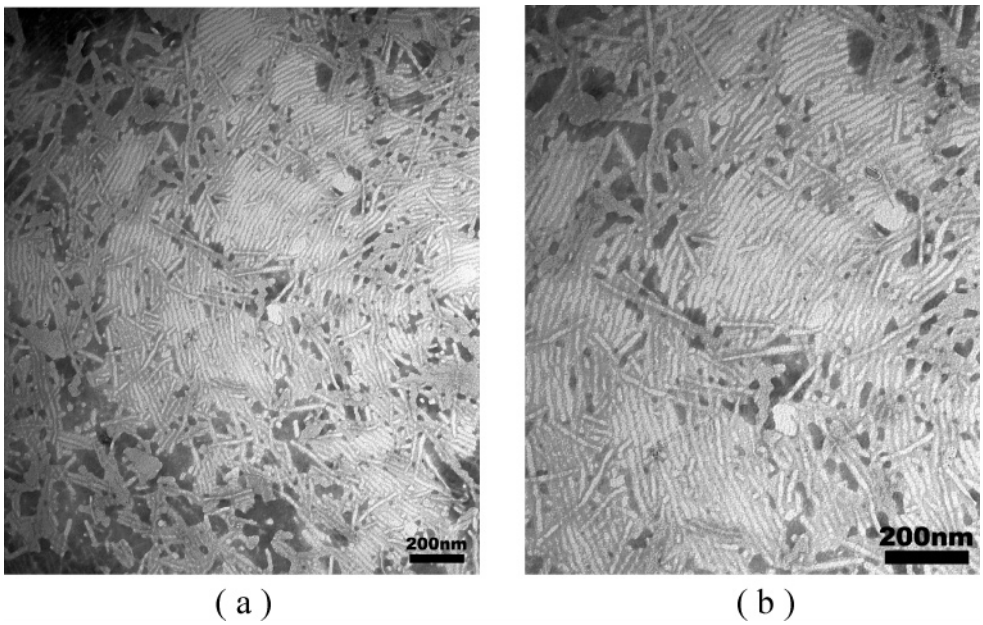

Figure 7. (a) TEM image of cylindrical micelles from (C-L)-E_{50} copolymer with concentration of 0.2 mg/mL; (b) a view recorded at higher magnification.

and swollen corona. Because of the incompatibility of A−B blocks in a highly selective solvent, both core and corona chains are considered to be grafted to the core−corona interface. High surface tension in the core−solvent surface favors more copolymers to be aggregated into one micelle in order to decrease the surface area per copolymer. However, as the micelles become larger, the densely grafted corona chains are more stretched because of an increase of the repulsion interaction. Consequently, it leads to a free energy penalty and thus restricting the aggregates' growth. The micellar equilibrium structure is determined by a balance between these two terms: the surface free energy associated with the core−solvent interface and the free energy penalty due to the stretching of the densely grafted corona blocks.

For the present P(CL-LLA)-*b*-mPEG copolymers, as described above, the micelles are prepared by first dissolving the block copolymers in DMF and subsequently slowly adding water to induce micelle formation, i.e., the aggregation of the P(CL-LLA) core blocks. At the initial stage of water addition, the quality of the solvent for P(CL-LLA) core blocks decreases slowly. At this stage, the system is both thermodynamically and kinetically controlled. When the content of water exceeds some critical value and finally the aggregates are isolated into water by dialysis, both of the lowered chain mobility and high enthalpy of crystallization of P(CL-LLA) core blocks make the system become kinetically inaccessible. Though in crystalline cores the configuration of the crystallizable core blocks is adjustable, there is no free energy change related with the configurational adjustments because the chain packing is ordered. Figure 8a shows a schematic illustration of the mechanism for micellization with cylindrical morphology. It involves a transition originated from a starlike crystalline−coil micelle, which exhibits a double stack of folded crystallized core surrounded by extended corona blocks. The final formation of cylindrical micelles is consistent with a strong competition between the energy of the crystalline core and chain stretching of the densely grafted mPEG corona. Because of the high surface tension between the hydrophobic core and water, more densely grafted

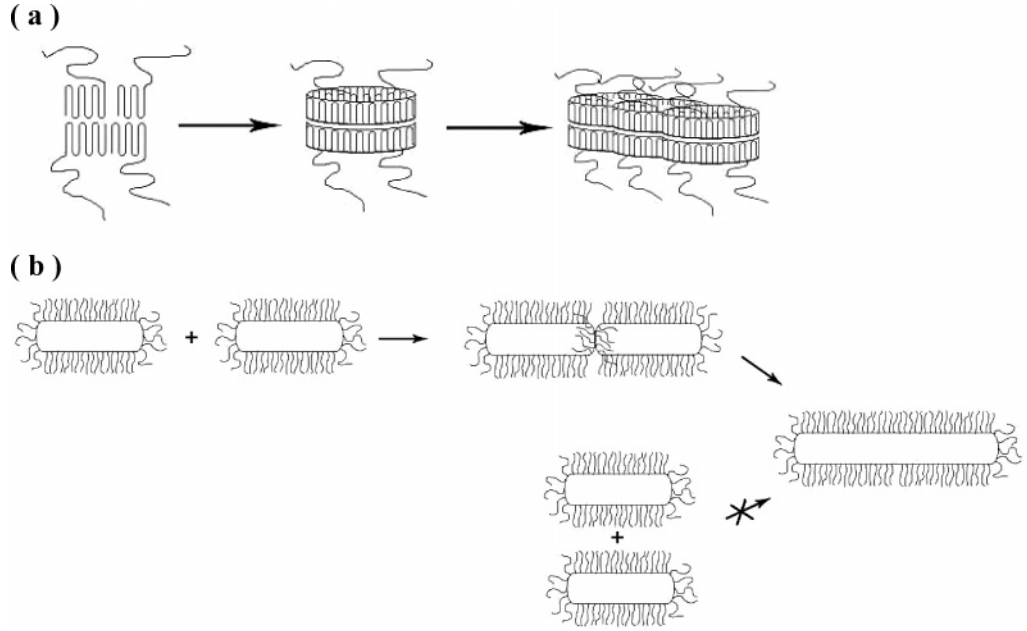

Figure 8. (a) Schematic illustration of the micellization with cylindrical morphology in solution and (b) the collision-reorganization mechanism forming extended micelles when the concentration increases.

mPEG chains is favored to a flat grafted layer in order to decrease the average area per corona chain, that is to say, a transition from a sphere to a lamellar or cylindrical morphology would be preferred. However, the entropy loss from the stretching of corona chains in the case of lamellar therefore will be excessively considerable. A cylindrical structure provides the best balance between these effects.

The cylindrical morphology of micelles in solution is also supported by the observation of extended micelles in the (C-L)-E_{50} case as the concentration increases (see back Figure 7). In Figure 8b, a schematic drawing of a collision−reorganization mechanism is shown. As discussed in the previous mechanism, the cylindrical micelle with a crystalline core is thermodynamically controlled in water. When the concentration of copolymers increases, the efficiency of approaching collisions of the micelles becomes higher, and this becomes greater during water evaporation. As pointed out previously, the spherical surface is less thermodynamically stable than the low-curvature flat surface with less area per corona chain. So once two short cylindrical micelles are too closer to resist the hydrophobic interaction, the morphological reorganization occurs, leading to an increase in the length of cylindrical micelles other than in the width.

Conclusion

The micellization phenomena of amphiphilic block copolymers based on methoxy poly(ethylene glycol) with either the crystalline or amorphous Poly(caprolactone-*b*-lactide) were studied. CMC values of the copolymers in this study are generally quite low, which indicates the potential of these copolymers performing as drug delivery carriers. Partition equilibrium coefficient (K_v) of pyrene in the micellar solution of P(CL-LLA)-*b*-mPEG copolymer was lower than that of P(CL-DLLA)-*b*-mPEG copolymer when the mPEG blocks were in the same length. In respect that the similar weight percentage of hydrophobic block for P(CL-LLA)-*b*-mPEG and P(CL-DLLA)-*b*-mPEG with the same length mPEG block, this depression of K_v values implies the difference in micellar core's physical structure between these two systems. From TEM images, the micelles assembled from P(CL-LLA)-*b*-mPEG were observed to take a cylindrical shape, which was independent of the investigated mPEG length, whereas those formed by P(CL-DLLA)-*b*-mPEG adopted a classical spherical shape. Based on the confirmation by DSC and WAXD analyses, the crystallization of the core-forming blocks is demonstrated to be the driving force governing the morphology of micelles in solution.

We propose a possible mechanism for the cylindrical morphology of P(CL-LLA)-*b*-mPEG micelles: a strong competition between the energy of the crystalline core and chain stretching of the densely grafted mPEG corona would be responsible for the formation of cylindrical micelles. Other ongoing experiments on the loading and releasing characteristics of P(CL-LLA)-*b*-mPEG and P(CL-DLLA)-*b*-mPEG systems as hydrophobic drug carriers are under investigation, particularly at the influence produced by the different physical state of micellar cores and micelle morphology on polymer−drug interactions. Those results will be published in forthcoming paper.

Acknowledgment. This project is financially supported by the National Nature Science Foundation of China (Grant Nos. 20474055 and 60373038).

References and Notes

(1) Hamley, I. W. *The Physics of Block Copolymers*; Oxford University Press: Oxford, 1998; Chapter 3, p 332.
(2) Allen, C.; Maysinger, D.; Eisenberg, A. *Colloids Surf. B: Biointerfaces* **1999**, *16*, 3−27.
(3) Torchilin, V. P. *J. Controlled Release* **2001**, *73*, 137−172.
(4) Shin, I. G.; Kim, S. Y.; Lee, Y. M.; Cho, C. S.; Sung, Y. K. *J. Controlled Release* **1998**, *51*, 1−11.
(5) Kim, S. Y.; Shin., I. G.; Lee, Y. M.; Cho, C. S.; Sung, Y. K. *J. Controlled Release* **1998**, *51*, 13−22.
(6) Yokoyama, M.; Satoh, A.; Sakurai, Y.; Okano, T.; Matsumura, Y.; Kakizoe, T.; Kataoka, K. *J. Controlled Release* **1998**, *55*, 219−229.
(7) Allen, C.; Yu, Y.; Maysinger, D.; Eisenberg, A. *Bioconjugate Chem.* **1998**, *9*, 564−572.
(8) Lele, B. S.; Leroux, J. C. *Macromolecules* **2002**, *35*, 6714−6723.
(9) Letchford, K.; Zastre, J.; Liggins, R.; Burt, H. *Colloids Surf. B: Biointerfaces* **2004**, *35*, 81−91.
(10) Dalhaimer, P.; Engler, A. J.; Parthasarathy, R.; Discher, D. E. *Biomacromolecules* **2004**, *5*, 1714−1719.

(11) Hans, M.; Shimoni, K.; Danino, D.; Siegel, S. J.; Lowman, A. *Biomacromolecules* **2005**, *6*, 2708−2717.
(12) Kallinteri, P.; Higgins, S.; Hutcheon, G. A.; Pourcain, C. B. S.; Garnett, M. C. *Biomacromolecules* **2005**, *6*, 1885−1894.
(13) Li, J.; Ni, X.; Li, X.; Tan, N. K.; Lim, C. T.; Ramakrishna, S.; Leong, K. W. *Langmuir* **2005**, *21*, 8681−8685.
(14) Garnier, S.; Laschewsky, A. *Macromolecules* **2005**, *38*, 7580−7592.
(15) Zhang, L.; Eisenberg, A. *Science* **1995**, *268*, 1728−1731.
(16) Zhang, L.; Eisenberg, A. *J. Am. Chem. Soc.* **1996**, *118*, 3168−3181.
(17) Yu, K.; Eisenberg, A. *Macromolecules* **1996**, *29*, 6359−6361.
(18) Ding, J.; Liu, G.; Yang, M. *Polymer* **1997**, *38*, 5497−5502.
(19) Bernheim-Groswasser, A.; Zana, R.; Talmon, Y. *J. Phys. Chem. B* **2000**, *104*, 4005−4009.
(20) Ravenelle, F.; Marchessault, R. H. *Biomacromolecules* **2003**, *4*, 856−858.
(21) Borsali, R.; Minatti, E.; Putaux, J.-L.; Schappacher, M.; Deffieux, A.; Viville, P.; Lazzaroni, R.; Narayanan, T. *Langmuir* **2003**, *19*, 6−9.
(22) Lei, L.; Gohy, J.-F.; Willet, N.; Zhang, J.-X.; Varshney, S.; Jerome, R. *Macromolecules* **2004**, *37*, 1089−1094.
(23) Minatti, E.; Viville, P.; Borsali, R.; Schappacher, M.; Deffieux, A.; Lazzaroni, R. *Macromolecules* **2003**, *36*, 4125−4133.
(24) Zhang, L.; Yu, K.; Eisenberg, A. *Science* **1996**, *272*, 1777−1779.
(25) Yu, G.-e.; Eisenberg, A. *Macromolecules* **1998**, *31*, 5546−5549.
(26) Zhang, L.; Eisenberg, A. *Macromolecules* **1999**, *32*, 2239−2249.
(27) Sidorov, S. N.; Bronstein, L. M.; Kabachii, Y. A.; Valetsky, P. M.; Soo, P. L.; Maysinger, D.; Eisenberg, A. *Langmuir* **2004**, *20*, 3543−3550.
(28) Vilgis, T.; Halperin, A. *Macromolecules* **1991**, *24*, 2090−2095.
(29) Cao, L.; Manners, I.; Winnik, M. A. *Macromolecules* **2002**, *35*, 8258−8260.
(30) Fu, J.; Luan, B.; Yu, X.; Cong, Y.; Li, J.; Pan, C.; Han, Y.; Yang, Y.; Li, B. *Macromolecules* **2004**, *37*, 976−986.
(31) Massey, J. A.; Temple, K.; Cao, L.; Rharbi, Y.; Raez, J.; Winnik, M. A.; Manners, I. *J. Am. Chem. Soc.* **2000**, *122*, 11577−11584.
(32) Fujiwara, T.; Miyamoto, M.; Kimura, Y. *Macromolecules* **2000**, *33*, 2782−2785.
(33) Fujiwara, T.; Miyamoto, M.; Kimura, Y.; Iwata, T.; Doi, Y. *Macromolecules* **2001**, *34*, 4043−4050.
(34) Fujiwara, T.; Kimura, Y. *Macromol. Biosci.* **2002**, *2*, 11−23.
(35) Feng, X.; Song, C.; Chen, W. *J. Polym. Sci. Polym. Lett. Ed.* **1983**, *21*, 593−600.
(36) Huang, M.; Li, S.; Vert, M. *Polymer* **2004**, *45*, 8675−8681.
(37) Pitt, C. G.; Jeffcoat, A. R.; Zweidinger, R. A.; Schindler, A. *J. Biomed. Mater. Res.* **1979**, *13*, 497−507.
(38) Zalipsky, S.; Gilon, C.; Zilkha, A. *Eur. Polym. J.* **1983**, *19*, 1177−1183.
(39) Bae, Y. H.; Huh, K. M.; Kim, Y.; Park, K. *J. Controlled Release* **2000**, *64*, 3−13.
(40) Wilhelm, M.; Zhao, C.-L.; Wang, Y.; Xu, R.; Winnik, M. A.; Mura, J.-L.; Riess, G.; Croucher, M. D. *Macromolecules* **1991**, *24*, 1033−1040.
(41) Stepanek, P., *Dynamic Light Scattering: The Method and Some Applications*; Clarendon Press: Oxford, 1993; Chapter 4, p 177.
(42) Moitzi, C.; Freiberger, N.; Glatter, O. *J. Phys. Chem. B* **2005**, *109*, 16161−16168.
(43) Yoshimura, S.; Shirai, S.; Einaga, Y. *J. Phys. Chem. B* **2004**, *108*, 15477−15487.
(44) Wu, J.; Pearce, E. M.; Kwei, T. K. *Macromolecules* **2002**, *35*, 1791−1796.
(45) La, S. B.; Okano, T.; Kataoka, K. *J. Pharm. Sci.* **1996**, *85*, 85−90.
(46) Hagan, S. A.; Coombes, A. G. A.; Garnett, M. C.; Dunn, S. E.; Davies, M. C.; Illum, L.; Davis, S. S. *Langmuir* **1996**, *12*, 2153−2161.
(47) Lee, S. C.; Chang, Y.; Yoon, J.-S.; Kim, C.; Kwon, I. C.; Kim, Y.-H.; Jeong, S. Y. *Macromolecules* **1999**, *32*, 1847−1852.
(48) Chang, Y.; Kwon, Y. C.; Lee, S. C.; Kim, C. *Macromolecules* **2000**, *33*, 4496−4500.

BM0601732